Sādhanā (2020)45:81
https://doi.org/10.1007/s12046-020-1323-6

© Indian Academy of Sciences

Hybrid controller for precision positioning application

A MUKHERJEE*, S K SHOME, P KARMAKAR and P BHATTACHARJEE

Information Technology, CSIR-Central Mechanical Engineering Research Institute, M G Road, Durgapur 713209, India
e-mail: a_mukherjee@cmeri.res.in

MS received 13 December 2019; accepted 17 January 2020

Abstract. In this paper, a precision positioning hybrid controller for long travel distance with submicron/nanometer resolution and accuracy is designed and developed. A hybrid control algorithm is designed to combine the coarse positioning system and a precision positioning system. The coarse positioning system consists of a linear stepper motor and coarse positioning controller, which is designed by microstepping with proportional-integral (PI) current feedback (MSPICF) control. In the precision positioning system, a piezoelectric actuator (PZA) is used. The mathematical model of the PZA has been represented by 2nd order mass-spring system with the Dahl hysteresis model and the model parameters are estimated by an autoregressive with exogenous terms (ARX) model identification technique using the input–output experimental data. The precision positioning controller designed by feedforward (FF) control which is the inverse of the mathematical model of the PZA and feedback (FB) control. The coarse, precision and hybrid controller is implemented using a low-cost DsPIC30F4012 microcontroller. Experiments have been performed to evaluate the performance of the controller.

Keywords. Microstepping control; stepper motor; feedforward control; feedback control; piezoelectric actuator.

1. Introduction

There has been rapid growth in the field of nanoscience and nanotechnology for the past two decades. Nanotechnology is a science that deals with the material and the control of that material in the order of 100 nm or less. Nano-surfaces having geometric structures smaller than 100 nm amplify certain chemical, physical and biological properties specific to the nanometer scale. The nano-surfaces behave differently with environments such as catalysts, magnetic energy, electronic emission/absorption, optical, antibacterial and pro-bacterial effects and so on, which have already been exploited for several high-end applications. Currently, the demand for the engineering of these nano-surfaces is growing rapidly. It can be used in many industrial fields, e.g. mechanics, electronics, chemistry, bioengineering, energy, information, and communication. The extreme precision positioning method has become a very important part for the development of precision machines such as the scanning tunneling microscope (STM) [1] and the atomic force microscope (AFM) [2] which have fundamentally altered the research in several areas like materials science, chemistry, biology, and physics. The nano-positioning tools are also required for the wafers positioning, semiconductor inspection systems, mask alignment, imaging and alignment in molecular biology, cell tracking and DNA analysis, nanomaterials testing, nanoassembly, manufacturing of micro/nano objects, optical alignment systems in space telescopes. This huge range of applications in diverse situations provides new challenges in the domain of control system for nano-positioning devices. With increasing miniaturization, the extreme-precision positioning systems with long strokes of several millimeters in nanometer-accuracy and resolution are becoming more and more attractive.

The piezoelectric actuator (PZA) is the most popularly used actuator demanding fast and high-resolution positioning systems [3–5]. The inherent characteristics of piezoelectric actuators make them most appropriate for fine, fast and very short range positioning applications. However for different applications, this short range ($\approx$ 100 μm) is not always sufficient. In [6], a double-stage arrangement is proposed to overcome the shortcomings of single PZA. In [7], a new actuator has been presented for a comparatively long operation range with a 10 nm step size by combining a PZA and pneumatic cylinder. A similar approach has been proposed by combining the PZA with a coarse voice-coil actuator for hard disk drives in [8, 9]. The control performance of a high-precision positioning table, driven by a hybrid actuator consist of PZA and voice-coil

*For correspondence
Published online: 27 March 2020

motors (VCMs) is presented in [10]. The hybrid actuator possesses both the features, i.e., a long operation ranges caused by the large stroke of VCM, and the actuation of PZA provide the ability of heavy load and high precision positioning. A new micro-gripper for micro-assembly and micro-manipulation is presented in [11], the new actuator is a combination of the coarse positioning system (thermal actuation) and the fine positioning system (piezoelectric actuation). A long travel motion with a resolution of 50 nm has been achieved by a linear stepping PZA comprise of two longitudinally bending hybrid transducers [12]. In [13], the author proposed a linear PZA functioning at inertial and direct actuation mode with high scan rate nanometer resolution, and large stroke length.

In this paper, it is proposed that along with the precision positioning actuator (piezo actuator) with nm accuracy, a coarse positioning actuator with μm accuracy has been combined to overcome the stroke limitation. There are quite a few options that can be used as a coarse positioning actuator e.g. DC servo motor, permanent magnet linear motors, linear switched reluctance motors, permanent magnet stepper motor, and voice coil motor. Considering the pros and cons of each actuator, it is decided to use permanent magnet stepper motors due to its cost and efficiency. Here, a stepper motor and a piezoelectric actuator are combined to achieve long travel range and submicron/nanometer accuracy and resolution. A new hybrid positioning control algorithm has been proposed and implemented using a low-cost DsPIC30F4012 microcontroller. First, the coarse positioning controller is designed and developed for a stepper motor by a micro-stepping with PI current feedback (MSPICF) controller and the precision positioning controller is designed by feedforward (FF) plus feedback(FB) controller for the PZA. The discrete mathematical model of the PZA has been developed by considering a mass-spring-damper (MSD) system along with the Dahl hysteresis model. The parameters of the piezoelectric actuator's model are evaluated by the model identification technique, namely ARX using the input–output experimental data. The FF controller is implemented by the inverse of the mathematical model of the PZA. The proposed hybrid control algorithm combines the controller of SM and PZA to achieve the desired performance. The remaining paper is arranged as follows. In section 2, the MSPICF control for stepper motor is discussed. The model identification technique of the piezoelectric actuator along with the design of the FF and FB control system is described in section 3. The proposed hybrid controller algorithm is discussed in section 4. Section 5 consists of experimental results, and conclusions are drawn in section 6.

2. Coarse positioning controller

The performance of the open-loop control system is considerably good in case of the permanent magnet stepper motor (PMSM). However, the standard PMSM has some inherent problems in precise positioning application at low speed due to oscillations of motor-shaft. Microstepping controller [14] was proposed and used to increase the positioning resolution as well as to improve the stability of the motion. PI feedback current control methods and speed profile algorithm have been designed and implemented for performance improvement of the microstepping controller. The motor produces positioning error due to the jerk during the start and stop. A speed profile is implemented in the controller where the motor slowly gains its final speed similarly the speed slowly reduces to zero. The micro-stepping PI current feedback controller (MSPICF) with a speed profile algorithm has been implemented in the DsPIC30F4012 microcontroller as shown in figure 1.

2.1 *Micro-stepping with PI current controller*

The phase currents of the stepper motor are [15].

$$i_a = I_p \cos(N\theta)$$
$$i_b = I_p \cos(N\theta)$$

Where i_a and i_b are the phase current, θ is the angular position of the rotor and I_p is the peak value of the phase current.

$$\text{Thus,} \quad I_p = \sqrt{(i_a^2 + i_b^2)}$$

The discrete-time PI current controller is designed and incorporated using DsPIC30F4012 microcontroller to maintain the desired current level at I_{pr} as follows

$$u(k) = K_p e(k) + Integral(k)$$

Where, $e(k) = I_{pr}(k) - I_p(k)$ and $Integral(k) = Integral(k-1) + K_i[(e(k) - e(k-1)]\frac{\Delta\tau}{2}.K_p$ and K_i are tunable proportional and integral gain respectively. $\Delta\tau$ is the sampling time. The integration of error is set as follows to avoid the integral wind-up.

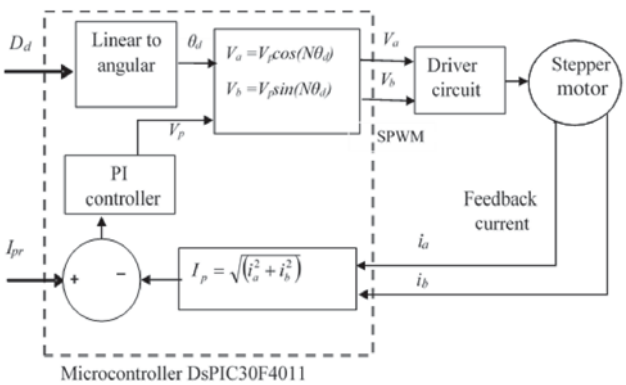

Figure 1. MSPICF control of stepper motor [15].

$$if\{(Integral(k) > Integral(\max))$$
$$or(Integral(k) < Integral(\min))\}$$

Then set, $\{Integral(k) = Integral(k-1)\}$

Here, a linear stepper motor has been used. The input of the controller is the desired position D_d (mm), so it is transformed into an equivalent desired angular position θ_d (rad). The phase voltages v_a and v_b are represented as $v_a = v_p \cos\theta_d$ and $v_b = v_p \sin\theta_d$.

3. Precision positioning controller

Here, the piezoelectric actuator has been used in the precision positioning controller. PZA is most popular and widely used in nano-positioning applications. PZA has many advantages such as very good operating bandwidth, compact design, generate large mechanical forces with small amounts of power. However, the PZA has the disadvantage of hysteresis, resonant frequency and creep, which can be overcome by proper control system design. Here first the mathematical model of the PZA is developed then the FF controller is designed by the inverse mathematical model of the PZA. The Precision positioning controller is developed by combining the FF controller with the PI feedback control and it is implemented in the DsPIC30F4012 microcontroller.

3.1 *Mathematical Model and Identification of Piezoelectric Actuator*

In the present research, the piezoelectric system is represented by a linear second order MSD system along with the nonlinear hysteresis effect. The mathematical model of the PZA is established as follows [16]

$$M\ddot{x} + D\dot{x} + Kx = Tu - F_h \tag{1}$$

$$\dot{z} = (A_h\dot{x})z + (B_h u_p)\dot{x} \tag{2}$$

$$F_h = C_h z \tag{3}$$

Where, M is the system mass, D denotes damping coefficient, K represents stiffness, T is the piezoelectric coefficient, u is the input voltage, x denotes displacement along the x-axis, and F_h is the hysteresis force. F_h can be expressed in state space form as follows

Where, $z = [p_1 \quad p_2]^T$ is the intermediate state vector, u_p is a constant [16], and the matrices are

$$A_h = \begin{bmatrix} 0 & 1 \\ -a_2 & -sign(\dot{x})a_1 \end{bmatrix}, \quad B_h = \begin{bmatrix} 0 \\ 1 \end{bmatrix},$$
$$C_h = [b_1 \quad sign(\dot{x})b_0] \tag{4}$$

Thus, using (2), (3) and (4), Dahl hysteresis non-linear force can be mathematically represented as follows.

$$\begin{aligned} \dot{p}_1 &= p_2\dot{x} \\ \dot{p}_2 &= -p_1 a_2\dot{x} - p_2 a_1 \mathrm{sgn}(\dot{x})\dot{x} + u_p\dot{x} \\ F_h &= p_1 b_1 + b_0 p_2 \mathrm{sgn}(\dot{x}) \end{aligned} \tag{5}$$

The hysteresis parameters a_1, a_2, b_0 and b_1 have been experimentally determined [16] using the following equations

$$a_1 = \frac{2}{(t_1 - t_2)} \ln \frac{H_1 - H_s}{H_2 - H_s} \tag{6}$$

$$a_2 = \frac{4\pi^2}{(t_1 - t_2)^2} + \frac{a_1^2}{4} \tag{7}$$

$$b_1 = G_{dc} a_2 \tag{8}$$

$$b_0 = S_0 \tag{9}$$

where H_1 is the 1st peak and H_2 is the 2nd peak height of the overshoot of the open loop step response of the PZA as shown in figure 2, t_2–t_1 is the time duration between occurrence of H_1 and H_2, the value of the steady state response is denoted by H_s, G_{dc} is the DC gain, and S_0 denotes the initial response slope.

For time domain step response, the DC gain, G_{dc} is represented by the ratio of H_s to the input step voltage and initial slope $S_0 = 0$. Thus, we have

$$a_1 = \frac{2}{(0.021 - 0.0150)} \ln\left(\frac{28.6 - 21.1}{26.4 - 21.1}\right) = 115.732$$

$$a_2 = \frac{4\pi^2}{(0.021 - 0.0150)^2} + \frac{115.732^2}{4} = 1098859.58$$

$$b_1 = G_{dc} * a_2 = (21.1/75) * a_2$$

$$b_0 = 0$$

A state space representation of the PZA together with the non-linear hysteresis force can be represented using the state vector

$$X = [x, \dot{x}, p_1, p_2]^T.$$

$$\begin{aligned} \dot{X} &= AX + Bu \\ Y &= CX \end{aligned} \tag{10}$$

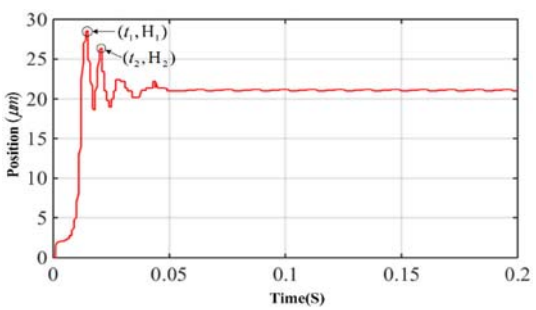

Figure 2. Open loop step response of the PZA for 75 V input.

$$\text{Where,} \quad A = \begin{bmatrix} 0 & 1 & 0 & 0 \\ -\frac{K}{M} & -\frac{D}{M} & -\frac{b_1}{M} & -\frac{b_0}{M}\text{sgn}(\dot{x}) \\ 0 & 0 & 0 & \dot{x} \\ 0 & u_p & -a_2\dot{x} & -a_1\dot{x}\text{sgn}(\dot{x}) \end{bmatrix},$$

$$B = \begin{bmatrix} 0 \\ \frac{T}{M} \\ 0 \\ 0 \end{bmatrix}, \quad \text{and} \quad C = [1 \quad 0 \quad 0 \quad 0] \tag{11}$$

The system represented in the discrete-time domain is more preferable than the system in the continuous-time domain for digital control. So, a discrete-time PZA model is derived from the continuous-time PZA model, by converting the differential equations (1)–(4) into difference equations. The following equations are written at kth time instant with sampling time $\Delta\tau$.

$$\dot{x}(t) = \frac{x(k+1) - x(k)}{\Delta\tau} \tag{12}$$

$$\ddot{x}(t) = \frac{\dot{x}(k+1) - \dot{x}(k)}{\Delta\tau} \tag{13}$$

Using (12), we get.

$$\ddot{x}(t) = \frac{x(k) - 2x(k-1) + x(k-2)}{\Delta\tau^2} \tag{14}$$

Using (12), (13), (14) and (1), the PZA model in the discrete-time domain can be represented as [17]

$$x(k) = Px(k-1) + Qx(k-2) + Ru(k) + SF_h(k) \tag{15}$$

Where, $P = \frac{\frac{2M}{\Delta\tau^2} + \frac{D}{\Delta\tau}}{\frac{M}{\Delta\tau^2} + \frac{D}{\Delta\tau} + k}$, $Q = -\frac{\frac{M}{\Delta\tau^2}}{\frac{M}{\Delta\tau^2} + \frac{D}{\Delta\tau} + k}$,

$$R = \frac{T}{\frac{M}{\Delta\tau^2} + \frac{D}{\Delta\tau} + k}, S = -\frac{1}{\frac{M}{\Delta\tau^2} + \frac{D}{\Delta\tau} + k}$$

Now, the continuous-time Dahl hysteresis force has been represented in the discrete time domain by substituting $\dot{z}(t) = \frac{z(k+1) - z(k)}{\Delta\tau}$, $z(k) = \begin{bmatrix} z_1(k) \\ z_2(k) \end{bmatrix}$ and $\dot{x}(t) = \frac{x(k+1) - x(k)}{\Delta\tau}$ in (2), (3), and (4), which yields

$$z_1(k) = z_1(k-1) + z_2(k)\{x(k) - x(k-1)\} \tag{16}$$

$$z_2(k) = \frac{z_2(k-1) + u_p\{x(k) - x(k-1)\} - a_2 z_2(k)\{x(k) - x(k-1)\}}{1 + a_1\{x(k) - x(k-1)\}\text{sgn}\left\{\frac{x(k) - x(k-1)}{\Delta\tau}\right\}} \tag{17}$$

$$F_h(k) = z_1(k)b_1\text{sgn}\left\{\frac{x(k) - x(k-1)}{\Delta\tau}\right\} b_0 z_2(k) \tag{18}$$

The discrete-time PZA model (15) can be expressed in Z-domain as

$$X(Z) = \frac{Z^2\{RU(Z) + SF_h(Z)\}}{Z^2 - PZ - Q} \tag{19}$$

The block diagram of the discrete-time PZA model and Dahl hysteresis model is shown in figure 3a and b respectively.

Several experimental input–output data have been used to identify the parameters of the transfer function using the ARX [18] regeneration model. The regressing model is defined as [17].

$$y(k) = \varphi^T\theta + e(k) \tag{20}$$

Where, $\varphi^T = [x(k-1), x(k-2), u(k), F_h(k)]$ and $\theta^T = [P, Q, R, S]$.

The identified parameters mentioned in table 1.

3.2 *Feedforward and feedback controller*

Feedforward (FF) control has the advantage of performance improvement without involving the stability issues related with feedback (FB) control design. However, it cannot account for modelling errors. Specifically, inversion-based FF controllers cannot rectify the tracking errors resulted from the plant uncertainties [19]. Thus, it is required to cascade the FB controller in combination with FF to minimize errors due to uncertainty in the system. The effect of cascaded FF and FB control improves the tracking performance compared to only FB control in the presence of uncertainties has been shown in [20]. FF and FB controllers can be cascaded to exploit the advantages of each control regime. In this scheme, the inverse mathematical model of

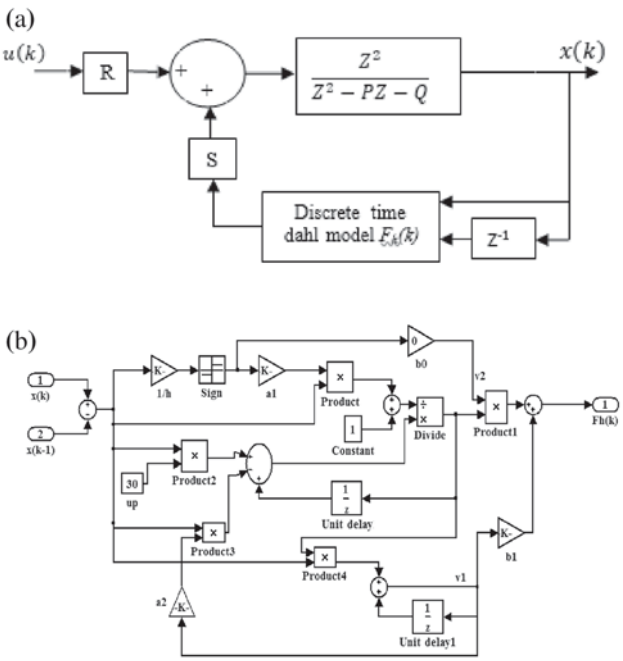

Figure 3. **a.** Block diagram of the PZA in the discrete domain. **b.** Block diagram of Dahl hysteresis model in discrete-time domain.

Table 1. Identified parameters of PZA model.

Sl. no.	Parameter	Value
1	P	0.4903
2	Q	0.4369
3	R	2.2023×10^{-8}
4	S	-5.6875×10^{-5}
5	a1	115.732
6	a2	1.098859×10^{6}
7	b1	3.09292×10^{5}
8	b0	0

the plant controller is used to mitigate the effect of the hysteresis in the feedforward part while the FB controller handles the external system disturbances and varying system dynamics, shown in figure 4.

The compensating input to mitigate the effect of hysteresis can be found using eq. (15).

$$u_{FF}(k) = P_1x(k) + Q_1x(k-1) + R_1x(k-2) + S_1F_h(k \quad (21)$$

Where, $P_1 = \frac{1}{R}$, $Q_1 = -\frac{P}{R}$, $R_1 = -\frac{Q}{R}$, $S_1 = -\frac{S}{R}$

The FB controller is designed by a PI position feedback controller. The position of the piezoelectric actuator has been measured by the attached SGS sensor with the PZA. The mathematical model of the SGS sensor is also obtained from the experimental input–output data through the model identification technique.

The feedforward controller is implemented using the DsPIC30F4011 microcontroller and DAC MCP4922. The feedforward controller is designed using input/output experimental data of the PZA, P841.20. The controller generates the control voltage as per the input desired distance. The control voltage is applied to the PZA after amplification of the signal by an amplifier. The displacement of the PZA is measured by a strain gauge sensor (SGS) attached to the PZA actuator. The SGS sensor output is displayed and measured by the display module, E-501.00.

4. Hybrid control structure

A hybrid control structure has been developed to achieve submicron/nanometer accuracy and resolution over large displacements of several centimeters. The hybrid

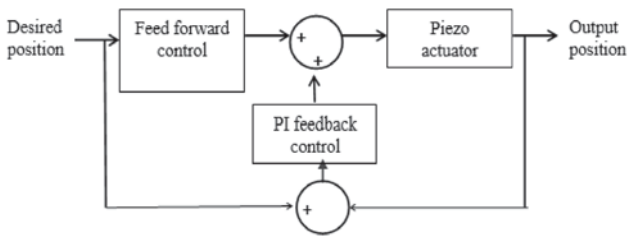

Figure 4. Block diagram of FF and FB controller for PZA.

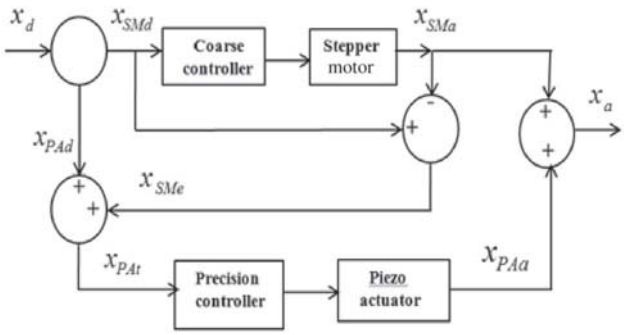

Figure 5. Hybrid control structure.

controller consists of two parts coarse positioning controller and precision positioning controller. In coarse positioning controller, micro-stepping control with 10,000 steps per revolution and driver circuit has been developed for the stepper motor to cover the long travel distance. And in precision positioning system, feedforward and feedback controller for piezoelectric actuator has been used been developed to achieve the submicron/nano travel resolution. The hybrid control structure integrates these two coarse and precision positioning controller to achieve long travel range as well as submicron/nano resolution. The implemented control structure is shown in figure 5 and discussed below.

In the hybrid control structure (figure 5) total desired distance x_d is given input to the controller. The distance in mm range up to 2nd decimal place is considered by the stepper motor x_{SMd}. An (10,000 ppr) encoder is attached to the stepper motor. From the encoder reading the actual distance travelled by the stepper motor x_{SMa} is found out also the error introduced by the stepper motor $x_{SMe} = (x_{SMd} - x_{SMa})$ is calculated. The remaining of total desired distance $x_{PAd} = (x_d - x_{PAd})$ after 2nd decimal place in mm unit (in μm range) is considered by the piezo actuator along with the error contributed by the stepper motor. So the total desired distance of the piezo actuator is $x_{PAt} = x_{PAd} + x_{SMe}$. The actual displacement of the piezo actuator x_{PAa} is measured by the embedded SGS sensor which is displayed and measured by the display module, E-501.00. So the actual distance travel by the hybrid structure is obtained as $x_a = x_{SMa} + x_{PAa}$. The flowchart of the hybrid control algorithm is given in figure 6.

5. Experimental results and discussion

For long travel range with micro/nano resolution, a hybrid controller using the stepper motor (M-168.22 s) and piezoelectric actuator (P841.20) is developed. The hybrid structure (shown in figure 5) is implemented in the DsPIC30F4011 microcontroller. The hybrid controller performances for different desired distances are plotted.

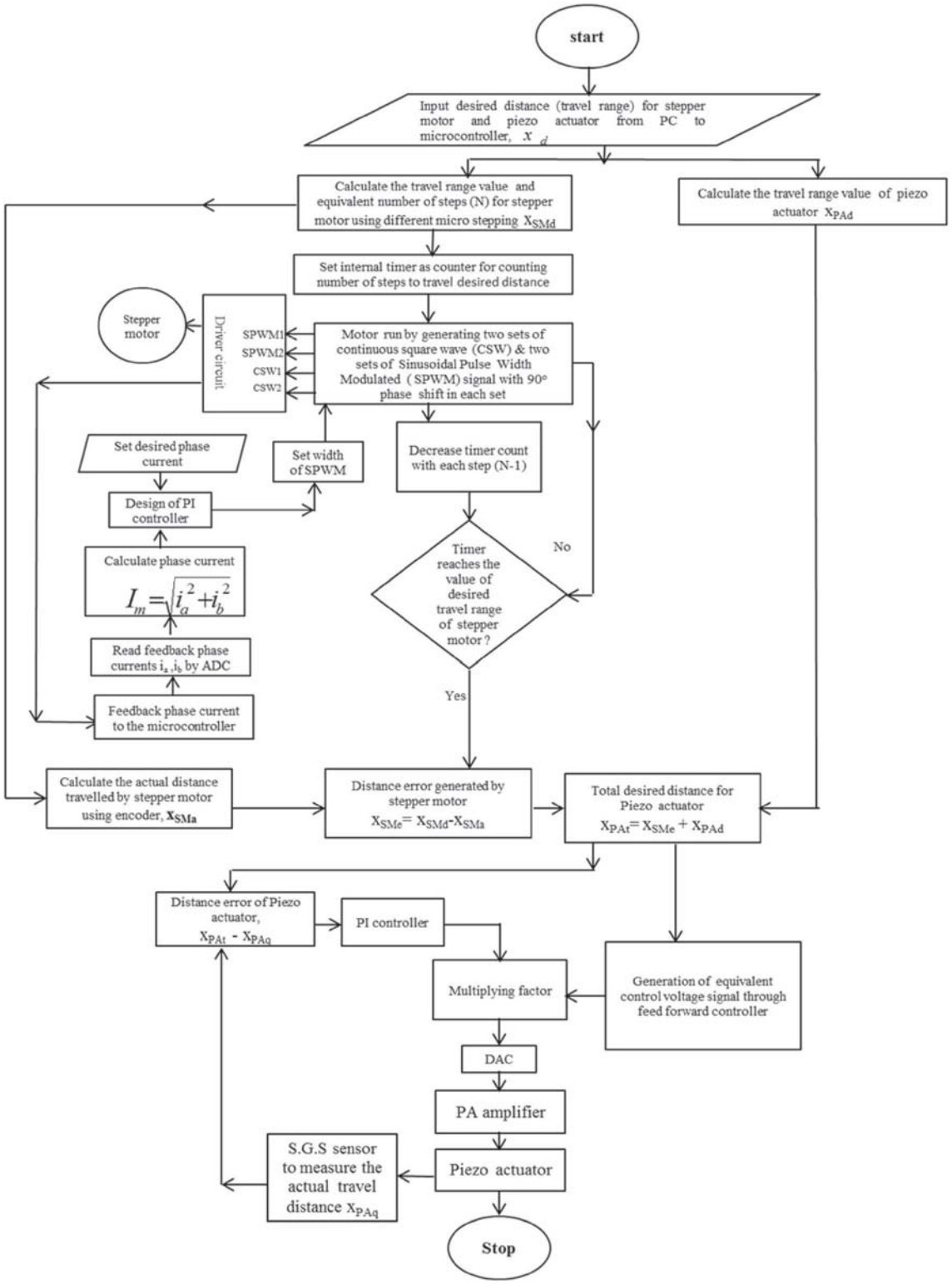

Figure 6. Flowchart of the hybrid controller.

The travel distance error vs. desired distance is shown in figures 7 and 8.

This hybrid structure can be used to control the position up to 25 mm (as maximum travel range of the motor

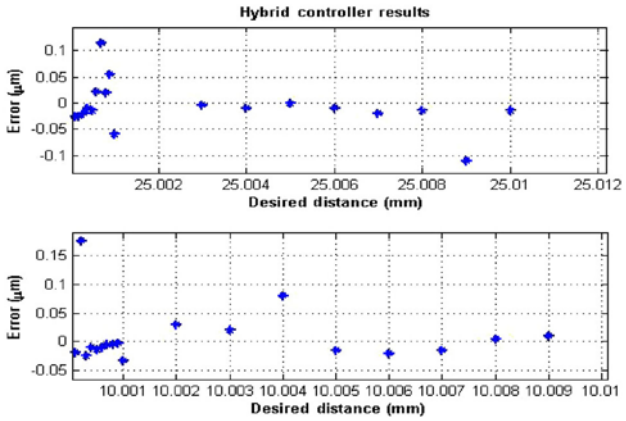

Figure 7. Position error at different desired distances using hybrid controller.

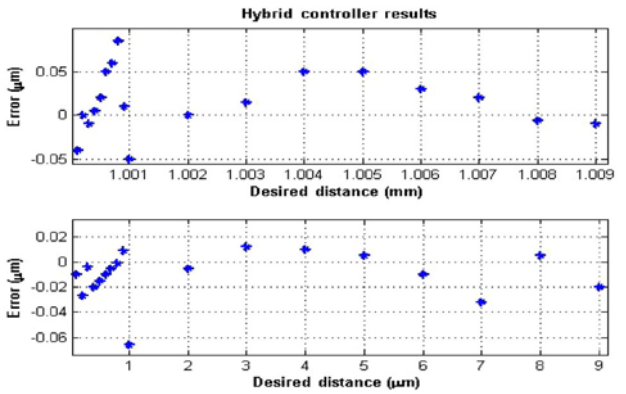

Figure 8. Position error at different desired distances using hybrid controller.

M-168.22 s is 25 mm) with a resolution and accuracy 0.1 μm.

6. Conclusion

A low-cost precision positioning controller is developed using the DsPIC30F4012 microcontroller for long travel range and submicron/nanometer accuracy and resolution. In this paper, three controllers have been designed and implemented namely coarse positioning controller, precision positioning controller, and hybrid controller. The coarse controller handles the long travel range, the precision positioning controller helps to achieve the submicron/nanometer resolution and accuracy, and the hybrid controller combines these two controllers to attain both the effects. The experimental results show that the hybrid precision positioning controller can be used to control the position up to 25 mm with submicron/nanometer resolution and accuracy. Here, linear stepper motor with its microstepping PI current feedback control is used as a coarse positioning system. The precision positioning controller consists of a piezoelectric actuator and its FF plus FB controller. The proposed controller can be used for positioning control up to 25 mm with 0.1 μm/100 nm resolution and accuracy.

References

[1] Binnig G and Rohrer H 1982 Scanning tunneling microscopy. *Helvetica Phys. Acta.* 55: 726–735

[2] Binnig G, Quate C F and Gerber C 1986 Atomic force microscope. *Phys. Rev. Lett.* 56 (9):930–933

[3] Hwang C-L, Che Y-M, Sin J. K. O. and Jan C 2005 Trajectory tracking of large-displacement piezoelectric actuators using a nonlinear observer based variable structure control. *IEEE Trans. Control Syst. Technol.* 13: 56–66

[4] Liu H, Lu B, Ding Y, Tang Y and Li D 2003 A motor-piezo actuator for nano-scale positioning based on dual servo loop and nonlinearity compensation. *Inst. of Physics Publishing, J. Micromech. Microeng.* 13

[5] Salapaka S, Sebastien A, Cleveland J P and Salapaka M V 2002 High bandwidth nano-positioner: a robust control approach. *Rev. Sci. Instrum.* 73: 3232-3241

[6] Michellod Y, Mullhaupt P and Gillet D 2006 Strategy for the Control of a Dual-stage Nano-positioning System with a Single Metrology. In: *Robotics, Automation and Mechatronics, 2006 IEEE Conference*, pp. 1–8

[7] Liu Y-T and Higuchi T 2001 Precision positioning device utilizing impact force of combined piezo-pneumatic actuator. *IEEE/ASME Trans. Mechatron.* 6(4): 467–473

[8] Mamun A Al, Mareels I, Lee T. H and Tay A 2003 Dual stage actuator control in hard disk drive—a review. In: *29th Annual Conference of the IEEE.*

[9] Schroeck S J, Messner W C and McNab R J 2001 On compensator design for linear time-invariant dual-input single-output systems. *IEEE/ASME Trans. Mechatronics* 6: 50–57

[10] Liu Y-T, Fung R-F and Wang C-C 2005 Precision position control using combined piezo-VCM actuators. *Precis. Eng.* 29(4): 411–422

[11] Rakotondrabe M and Ivan I A 2011 Development and force/position control of a new hybrid thermo-piezoelectric microgripper dedicated to micromanipulation tasks. *IEEE Trans. Autom. Sci. Eng.* 8(4): 824–834

[12] Shen Q, Liu Y, Wang L, Liu J and Li K 2018 A long stroke linear stepping piezoelectric actuator using two longitudinal-bending hybrid transducers. *Ceram. Int.* 44(1): 104–107

[13] Deng J, Chen W, Li K, Wang L and Liu Y 2019 A sandwich piezoelectric actuator with long stroke and nanometer resolution by the hybrid of two actuation modes. *Sensors Actuators A Phys.* 296(1): 121–131

[14] Kim W, Choi I and Chung C 2010 Lyapunov-based control in microstepping with a nonlinear observer for permanent magnet stepper motors. In: *Proceedings American Control Confernece*, pp. 4313–4318

[15] Mukherjee A, Karmakar P, Shome S K, Sen S and Datta U 2016 Precision positioning system for long travel range and submicron resolution. In: *2nd International Conference on Control, Instrumentation, Energy & Communication (CIEC), Kolkata, 2016.* pp. 83–87

[16] Xu Q and Li Y 2010 Dahl model-based hysteresis compensation and precise positioning control of an XY Parallel Micromanipulator with piezoelectric actuation. *J. Dyn. Syst. Meas. Control ASME*

[17] Shome S K, Mukherjee A, Karmakar P, Datta U 2018 *Sādhanā* 43: 158

[18] Broersen P M T and Waele S D 2005 Automatic identification of time-series models from long autoregressive models. *IEEE Trans. Instrum. Meas.* 54(5): 1862–1868

[19] Zhao Y and Jayasuriya S 1995 Feedforward controllers and tracking accuracy in the presence of plant uncertainties. *ASME J. Dyn. Syst., Meas. Control.* 117: 490–495

[20] Devasia S 2002 Should model-based inverse inputs be used as feedforward under plant uncertainty. *IEEE Trans. Autom. Control*. 47(11): 1865–1871